

Performance of PV Grid-Connected System Under Grid Failure

Mouhanned Brahim^{***‡}, Jamel Belhadj^{***}

*University of Tunis El Manar

**University of Tunis, ESSTT-DGE

(mouhannedbrahim@gmail.com, jamel.Belhadj@esstt.mu.tn)

[‡]Corresponding Author; Mouhanned BRAHIM, University of Tunis El Manar, LSE-ENIT, BP 37 Le Belvédère 1002, Tunis, Tunisia, mouhannedbrahim@gmail.com

Received: 15.09.2013 Accepted: 13.10.2013

Abstract- A great deal of research is being carried out to ameliorate the performance of photovoltaic (PV) grid-connected systems. This paper shows the performance of a 1kW PV grid-connected system under grid failure. Among grid faults, islanding operation mode and grid voltage sags are tested with the proposed system. Hysteresis current control combined with active Islanding Detection Methods (IDMs) are developed to determine the effectiveness of the single phase full bridge inverter to detect islanding. Single Phase Induction Motor (SPIM) is taken as local load to test the grid voltage sag conditions. Theoretical, simulations, and experimental result shows the performance of the proposed system.

Keywords- PV, Grid failure, IDMs, Voltage sags, SPIM

1. Introduction

The world-wide installed PV generators was rapidly growth, due to the competitiveness of this technology. PV electricity is an attractive solution especially for the remote areas not served by the power grid [1].

However, a number of issues need to be resolved before PV technology can reach its full potential; the design of reliable power converter interfaces and the development of suitable control laws to protect related equipment, local loads, and utility service personnel.

Among the problems that can be encountered for PV grid-connected systems, islanding operation mode; it occurs when a section of the utility system is isolated from the main utility voltage source while the PV generator continues to feed the utility lines in the isolated section [2]. This phenomenon can cause safety problems. Therefore, anti-islanding protection is required for connecting to the utility grid via an anti-islanding inverter (IEEE Std. 929-2000) and has undergone extensive study and discussion [2].

Grid voltage sag can also perturb the PV grid-connected system. This is defined as short duration reduction in RMS voltage.

In this paper, a 1 kW PV power generation system connected to the grid is proposed. Slip Mode phase Shift (SMS) and Active Frequency Drift (AFD) islanding detection methods are developed to detect the island operation mode.

The effectiveness of the SMS and AFD IDMs is analyzed using the concept of the Non Detection Zone (NDZ) in the quality factor Q_f and resonant frequency f_0 (Q_f versus f_0) space.

Single Phase Induction Motor (SPIM) is taken as local load to show the performance of the proposed system under grid voltage sags.

Theoretical analysis, simulation, and experimental results are presented

2. Proposed System

Figure 5 shows the synoptic of the PV grid-connected system. It consists of PV generator feeding a single phase full bridge inverter followed by a line transformer for the voltage amplification and galvanic isolation. The PV inverter will handle both, the DC to AC conversion and the MPPT. First

order filter (r,L) is used as output filter to decrease the Total Harmonics Distortion (THD) of the output current and voltage. Parallel RLC load is taken as local load.

2.1. PV panel and MPPT Algorithm

Photovoltaic arrays present a nonlinear I-V characteristic with several parameters that need to be adjusted from experimental data of practical devices [3]. Figure 1 and 2 shows the I-V and P-V characteristics of the chosen PV generator

As the PV panel operates at its highest efficiency at the MPP, a method should be applied on the PV panel control system to extract the maximum power. Usually, the nature of these methods is based on an algorithm which takes measurement and does some actions to extract as much power as possible from PV panel. In this paper, the Perturb and Observe (P&O) method was applied in order to track the MPP. The MPPT algorithm generate the current magnitude at the MPP. This amplitude is used as peak reference current (I_{refmax}) for the hysteresis controller [4].

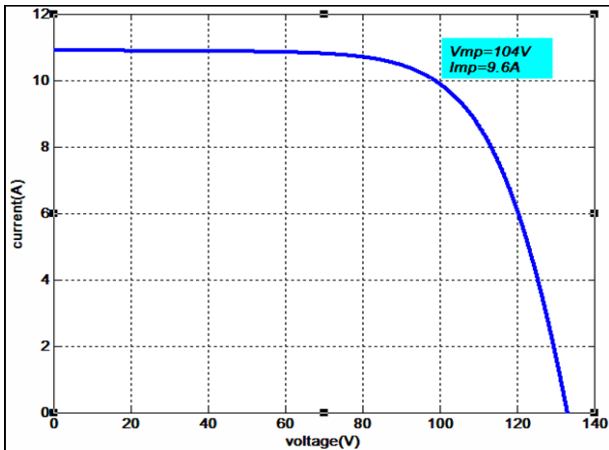


Fig. 1. I-V characteristics of PV generator

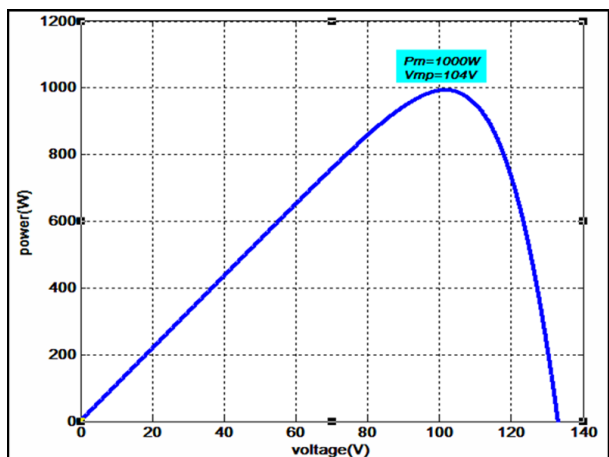


Fig. 2. P-V characteristics of PV generator

2.2. Normal Operation Mode

The output inverter current must be controlled to be in phase with the voltage at the point of common coupling V_{PCC} ,

so that the system works with unity power factor. As shown in figure 5, f_{PCC} and RMS detection blocks gives the phase angle of the PCC voltage (θ). This angle is used to generate the reference current for the hysteresis control

$$I_{ref} = I_{refmax} \sin(\theta) \tag{1}$$

As mentioned above I_{refmax} will be given by the MPPT controller. The actual output current (I) will be compared with the tolerance band around the reference current.

2.3. IDMs control loop

The inverter is controlled to detect islanding, when the grid is disconnected and to stop supplying the load and the grid. This technique is based on the detection of the Common Coupling Voltage V_{PCC} Frequency f_{PCC} for each zero crossing [5].

- Frequency and RMS detection

The islanding can be detected using the feedback from the PCC voltage at the previous cycle. When islanding occurs, the voltage frequency and magnitude deviate from the rated values. Therefore, the voltage frequency f_{PCC} for each zero crossing is detected and the RMS value is calculated.

- UVP/OVP and UFP/OFD

An Under/Over voltage and Under/Over frequency protection block is used to compare the RMS and the frequency values of the voltage at the Pcc to the thresholds values corresponding to the IEEE standards (IEEE std 929-2000). As a result, this block will generate a fault signal when the f_{PCC} or the RMS values exceed the fixed limits.

- Active Frequency Drift (AFD)

In some cases, although the variations of voltage and frequency are within the fixed limits, the islanding can occur and the inverter fails to detect it.

To overcome this problem, active IDMs use a variety of methods to inject a disturbance in the PCC voltage magnitude and frequency. Allowing the inverter to detect islanding.

The AFD rely in the injection of frequency drift at the output current to leads the PCC voltage by a small angle θ_{AFD} proportional to $t_z/2$ as shown in figure 3 [6] . The phase angle θ_{AFD} can be calculated as function of the frequency drift:

$$\theta_{AFD} = \pi f t_z = \pi f \left(\frac{1}{f} - \frac{1}{f + \delta f} \right) = \frac{\pi \delta f}{f + \delta f} \tag{2}$$

Where: δ_f is the amount of frequency drift.

The current frequency will be higher than the PCC voltage frequency at the previous cycle by a frequency drift ($f_k = f_{k-1} + \delta_f$). Therefore, the output inverter current can be given by:

$$i = I_{refmax} \sin[2\pi(f + \delta f)t] \tag{3}$$

- Slip Mode phase Shift (SMS)

SMS IDM rely in the injection of a phase shift in the inverter output current to create an abnormality in the PCC with keeping a unity power factor and a tolerable THD. The reference inverter current can be given by [7]:

$$i = I_{refmax} \sin[2\pi ft + \theta_{SMS}] \quad (4)$$

The phase shift is controlled to be a sinusoidal function of the PCC voltage frequency from the rated grid frequency:

$$\theta_{SMS} = \frac{2\pi}{360} \theta_{max} \sin\left(\frac{\pi}{2} \frac{f-f_g}{f_{max}-f_g}\right) \quad (5)$$

θ_{max} : Maximum phase shift in degree (°)

f_{max} : Frequency at θ_{max}

f_g : Rated grid frequency

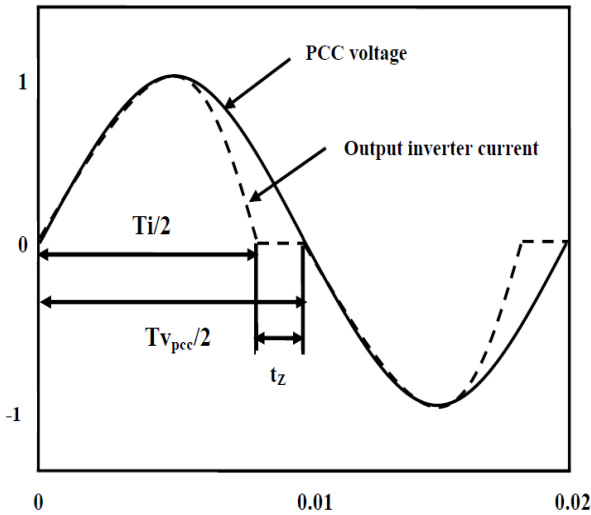


Fig. 3. Voltage and current waveforms using AFD

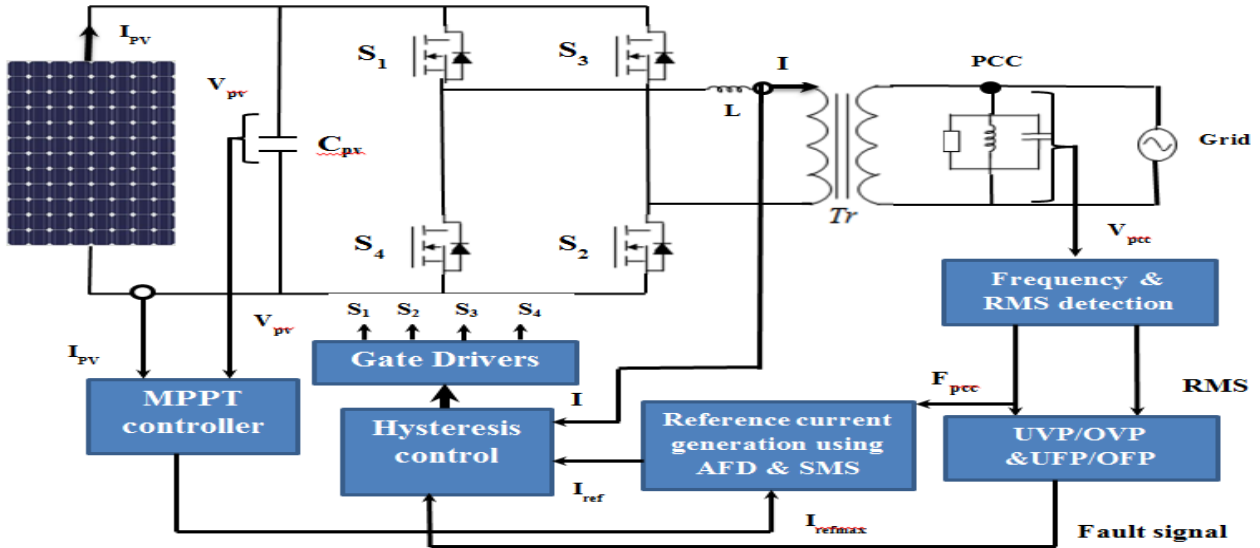


Fig. 5. The proposed controller for the PV grid connected system

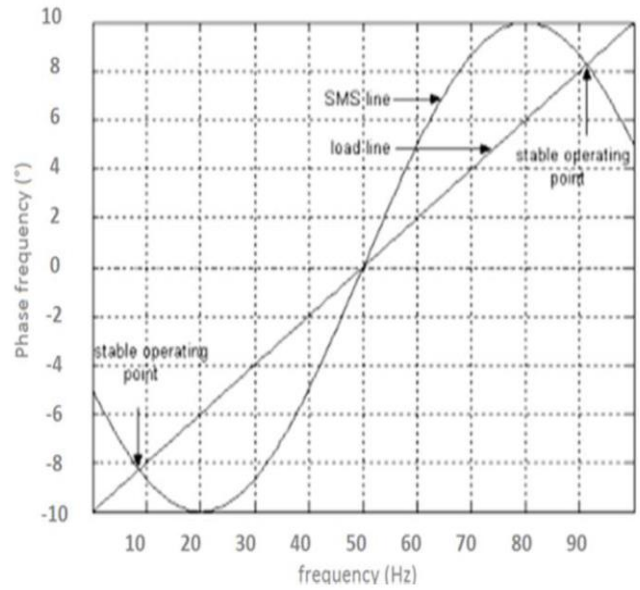


Fig. 4. SMS and load line response curves

3. Non Detection Zone (NDZ) of IDMs

NDZ is one of the most indexes to assess the effectiveness of the IDMs. This is defined as a range in which the IDMs fail to detect islanding. In the past, the NDZ have been defined in a power mismatch space (ΔP versus ΔQ). However, using NDZs in the power mismatch space is not adequate for assessing the performance of the active IDMs because for a given reactive power mismatch different combinations of R, L and C are possible. Some of these combinations result in islanding whereas others do not [8].

SMS and AFD IDMs employ a strategy to drift the frequency of the islanded system and trip the UFP/OFD since a significant active power mismatch is required to trip the UVP/OVP devices. The frequency of an islanded system with an unity power factor inverter is strongly affected by the load resonant frequency f_0 . If no disturbances are introduced, the frequency of the islanded system f_{is} will be the same as the resonant frequency since f_0 is the only frequency that satisfies $Q_{load} = Q_{pv} = 0$. Alternatively, the load phase angle should be equal to the phase between the output inverter current and the load voltage while the load phase angle is affected by the load quality factor Q_f . Therefore, $Q_f V_s f_0$ load-parameter space is a good choice for showing the NDZs and to assess the IDMs effectiveness [8].

3.1. NDZ of AFD IDM

The inverter phase angle can be defined as function of the quality factor Q_f and resonant frequency f_0 by [8]:

$$\theta_{inv} = \tan^{-1} \left[Q_f \left(\frac{f}{f_0} - \frac{f_0}{f} \right) \right] \tag{6}$$

The resolution of equation (6) gives

$$f^2 + \frac{\tan \theta_{inv}(f) f}{Q_f} f_0 - f_0^2 = 0 \tag{7}$$

Then the resonant frequency f_0 which causes islanding can be solved as a function of the islanding frequency f_{is} and the inverter equivalent angle.

$$f_0 = \frac{f_{is}}{2Q_f} \left(-\tan \theta_{inv}(f_{is}) + \sqrt{\tan^2 \theta_{inv}(f_{is}) + 4Q_f^2} \right) \tag{8}$$

For the AFD IDM, it was shown that the angle between the fundamental inverter current and the PCC voltage is given by

$$\theta_{AFD} = \frac{\pi \delta_f}{f + \delta_f} \tag{9}$$

By substituting equation (10) into (9) and replacing the islanding frequency by the threshold frequency. The boundary of the NDZ of the AFD IDM will be obtained by:

$$f_{0max} = \frac{f_{max}}{2Q_f} \left(-\tan \theta_{AFD}(f_{max}) + \sqrt{\tan^2 \theta_{AFD}(f_{max}) + 4Q_f^2} \right) \tag{10}$$

$$f_{0min} = \frac{f_{min}}{2Q_f} \left(-\tan \theta_{AFD}(f_{min}) + \sqrt{\tan^2 \theta_{AFD}(f_{min}) + 4Q_f^2} \right) \tag{11}$$

Therefore, the NDZs of the AFD IDM can be plotted with different values of δ_f as shown in figure 6.

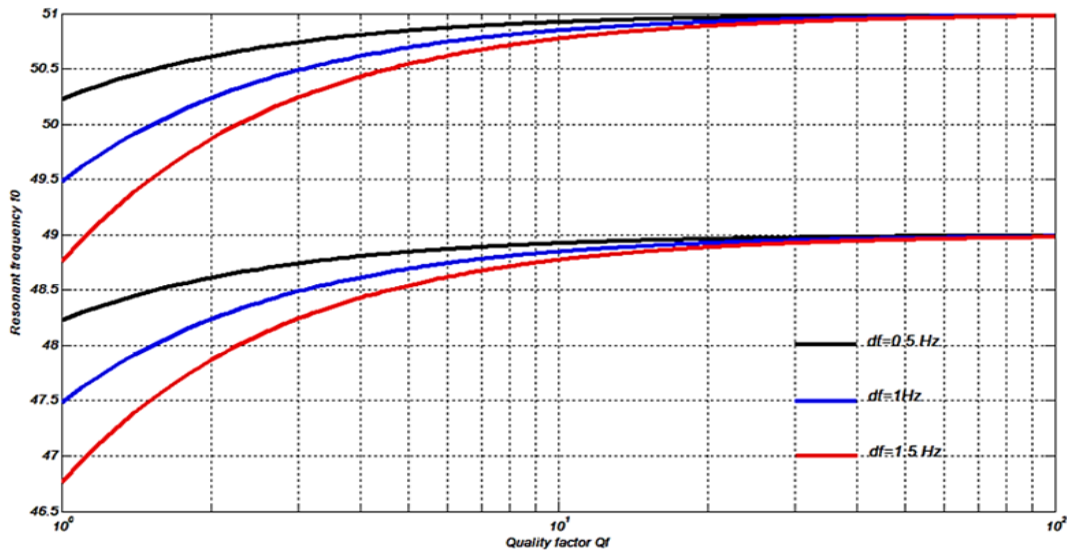


Fig. 6. NDZs of AFD IDM for different values of

There one sees that the main effect of AFD (injecting) is to shift the NDZ to lower values of f_0 as δ_f increases. From figure 6, with $Q_f = 2.5$ and $\delta_f = 0.5 \text{ Hz}$, this method will fail to detect islanding for load with $48.98 \text{ Hz} < f_0 < 50.2 \text{ Hz}$. It fail to detect islanding for load with $48.7 \text{ Hz} < f_0 < 49.8 \text{ Hz}$ when $\delta_f = 1 \text{ Hz}$, if δ_f increase to 1.5 Hz , the NDZ is for $48.3 \text{ Hz} < f_0 < 49.6 \text{ Hz}$ with load quality factor equal to 2.5 . One can sees also that with higher values of quality factor, the capability of islanding detection decrease for load with resonance frequency around line frequency (50Hz).

3.2. NDZ of SMS IDM

The NDZ of the SMS IDM can be determined with a similar analyzes method. The phase angle of the output inverter current is given by equation (6) mentioned above.

The resulting NDZ of SMS IDM is shown in figure 6 for different values of θ_{max} . One can see that as θ_{max} decreases, the quality factor for which the islanding cannot be detected also decreases. Where, for $f_{max} - f_g = 3 \text{ Hz}$, the SMS fail to detect islanding with load quality $Q_f > 2.7$ if $\theta_{max} = 12^\circ$. However, the value of the maximum phase shift θ_{max} is

limited by the phase angle between the output inverter current and the voltage at the PCC ($PF \approx 1$).

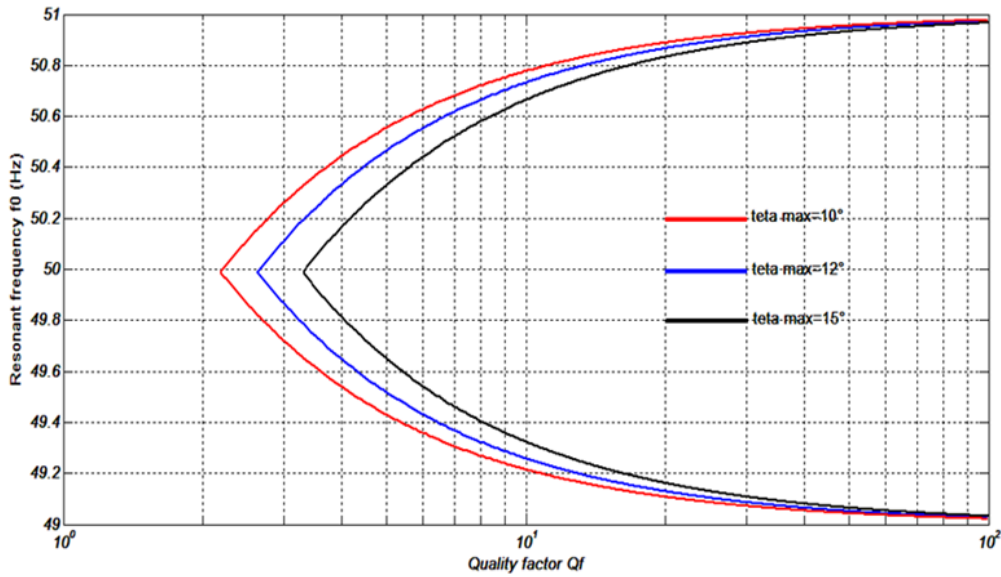


Fig. 7. NDZs of SMS IDM for different values of θ_{max}

Table 1. Parameters of photovoltaic generator at nominal operating conditions

N_{ser}	6
N_{par}	2
$I_{sc,n}$	10.85A
$V_{oc,n}$	133.2V
I_{mp}	9.68A
V_{mp}	104V
P_{max}	1 kW

4. Simulations

Simulations results are presented to verify the effectiveness of the proposed controller both for the normal operation mode and the islanding detection. Figure 8 shows the output inverter current and the voltage at PCC. One can see that the inverter operate with unity power factor and THD around 3.36 %.

- AFD IDM

The AFD is implemented for the frequency drift $\delta_f = 1.5\text{Hz}$. The local load parameters are $R=17.7 \Omega$, $L= 22.5 \text{mH}$, $C= 450 \text{uF}$ which gives a resonant frequency $f_0 = 50\text{Hz}$ and quality factor $Q_f = 2.5$. The grid breaker is opens at $t=0.1 \text{s}$, i.e. grid disconnected and islanding is detected at $t=0.338 \text{s}$.

Figure 11 shows the reference current generated by AFD IDM, from this figure one can see the dead time t_z which cause the abnormality at the PCC. As shown in figure 12, signal fault is generated to shut-down the inverter. The output inverter current and the voltage at the PCC are set to zero when the inverter stop energized the utility.

- SMS IDM

Similar tests were run for the PV grid-connected system using SMS IDM with

$\theta_{max} = 12^\circ$ and $f_{max} - f_g = 3\text{Hz}$. The local load parameters are $R=17.7 \Omega$, $L= 22.5 \text{mH}$, $C= 450 \text{uF}$ which gives a resonant frequency $f_0 = 50\text{Hz}$ and quality factor $Q_f = 2.5$. The grid is disconnected at $t=0.1 \text{s}$ and SMS IDM detect islanding at $t=0.472\text{s}$. Figure 13 shows the time domain response of the system

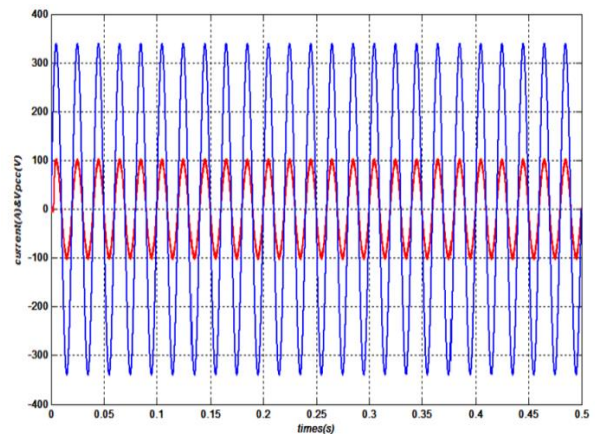


Fig. 8. V_{Pcc} & output current

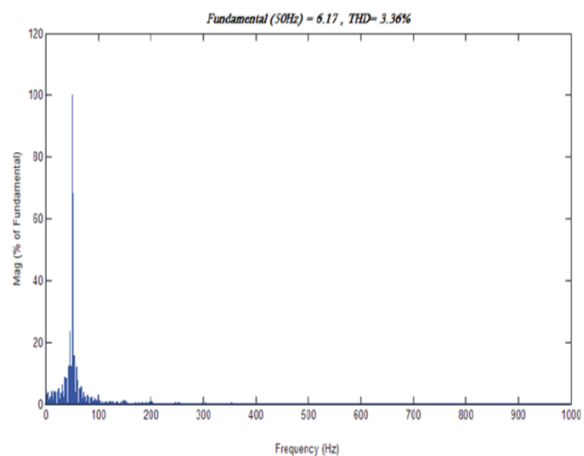


Fig. 9. THD of the output current

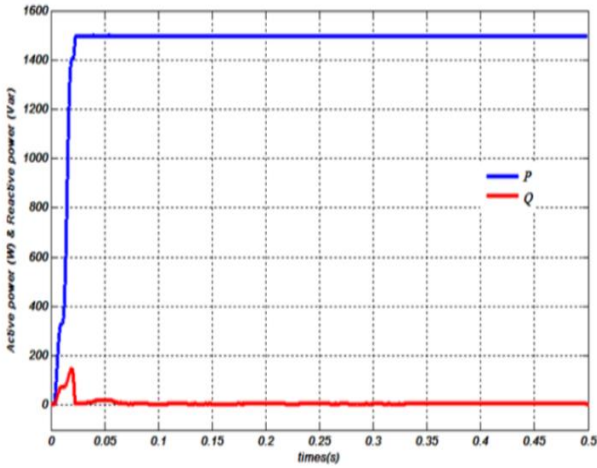


Fig. 10. Active & Reactive power

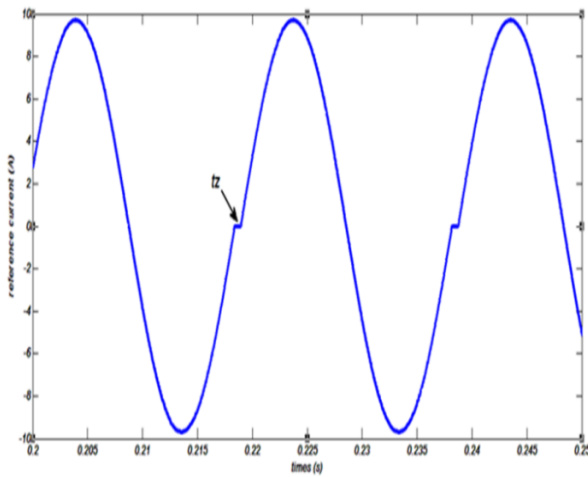


Fig. 11. AFD reference current

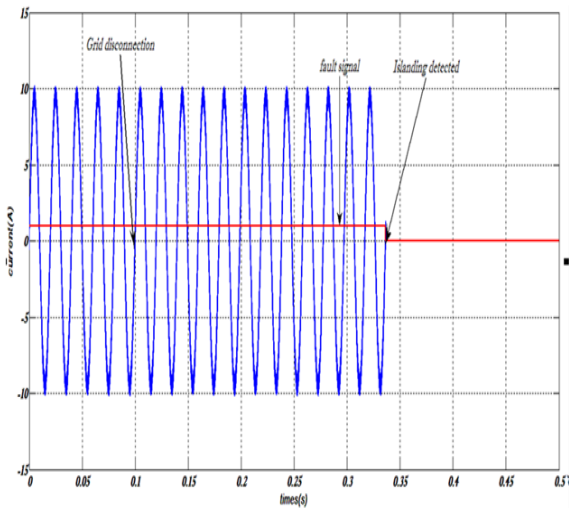


Fig. 12. Output current & signal fault

In order to verify the NDZs for each islanding detection method, several simulations are implemented with different load parameters. A comparison between the theoretical and simulation results for the NDZs of the AFD ($\theta_f = 1.5\text{Hz}$) and SMS ($\theta_{\max} = 12^\circ$) IDM are shown respectively in figure 14 and 15.

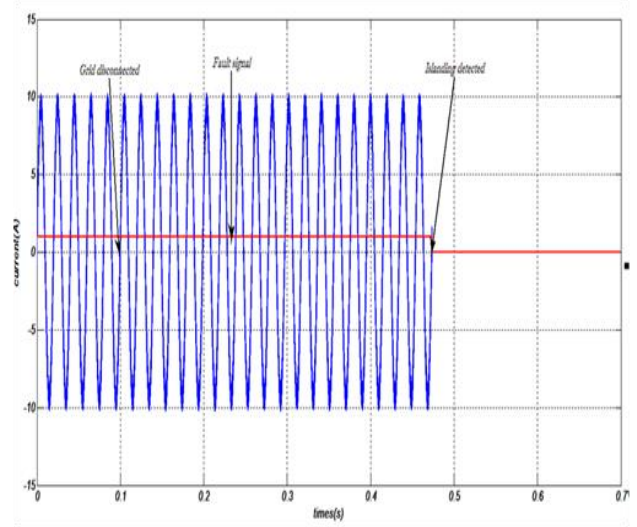


Fig. 13. Output current & signal fault

5. Performance of PV Grid-Connected System Under Grid Voltage Sags

Among problems that can be encountered in PV grid-connected systems, the grid voltage sags. This is defined as a short duration reduction in RMS voltage. It can occur at any instant of time, with amplitudes ranging from 10% to 90% and a duration lasting for half a cycle to one minute [9].

The same architecture of PV grid connected system is simulated. But, Single Phase Induction Motor (SPIM) is taken as local load instead of parallel RLC load to show the main effect of voltage sags. Grid voltage sags with different depth and durations are created, these are showing in simulation results. 50% and 80% voltage sags are simulated with different durations. One can see that the main effects of voltage sag are the SPIM speed losses and the peak load current. Moreover, as the voltage sag duration increases, the SPIM is more affected. The significantly speed losses can lead to a change of rotation direction as shown in figure 17, which can be a dangerous result from some application like water pumping or compressor.

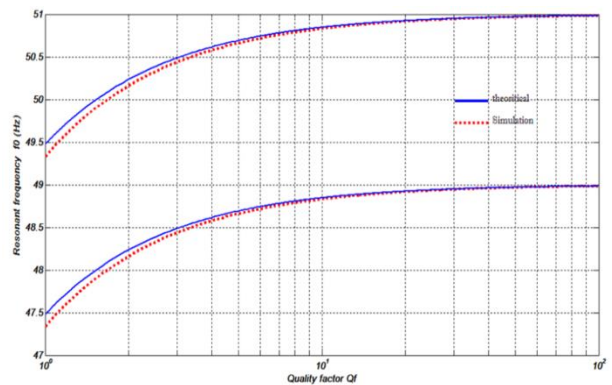


Fig. 14. NDZs of AFD

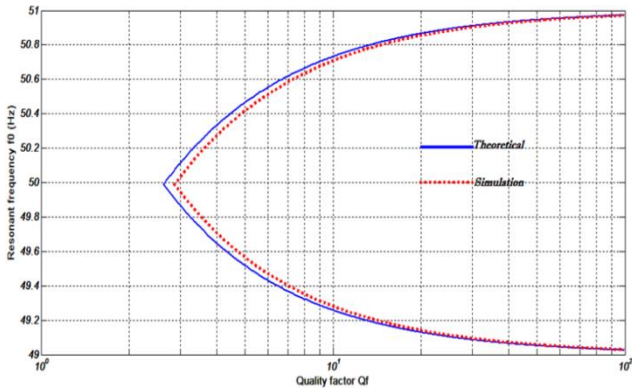


Fig. 15. NDZs of SMS

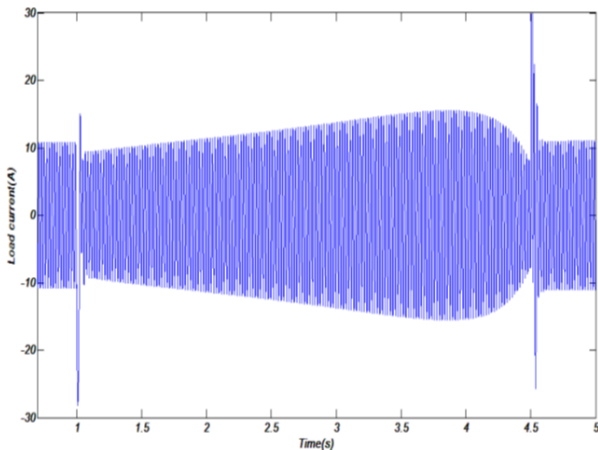


Fig. 16. Load current (80%, 3.5s)

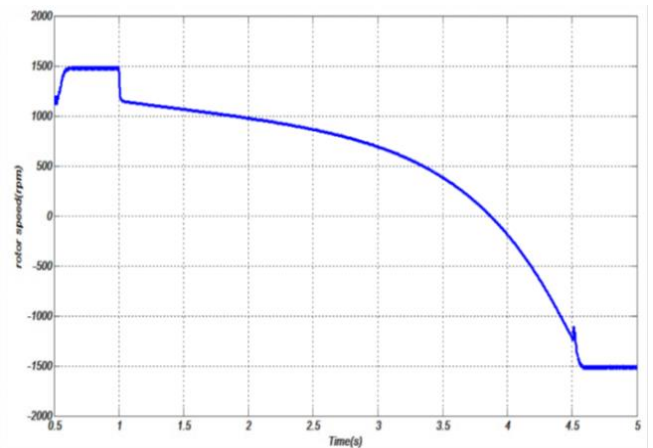


Fig. 17. Motor speed (80%, 3.5s)

6. Experiment Set

In the same context, an experimental single phase multilevel inverter (figure 18) is developed allowing the connection of PV panels to the grid and to verify the proposed control. The control algorithm is implemented in C language and computations are performed by a dSpace dS1104 controller board. The sampling period is fixed to 70µs. For each period, an interruption starts and the proposed control determines the switching states to apply. The numeric outputs of the dS1104 are used to control the converter drivers. Figure 20 shows the experimental inverter output current compared to the generated reference current. The output inverter voltage levels are given by figure 19. It can be noted that four voltage levels can be obtained

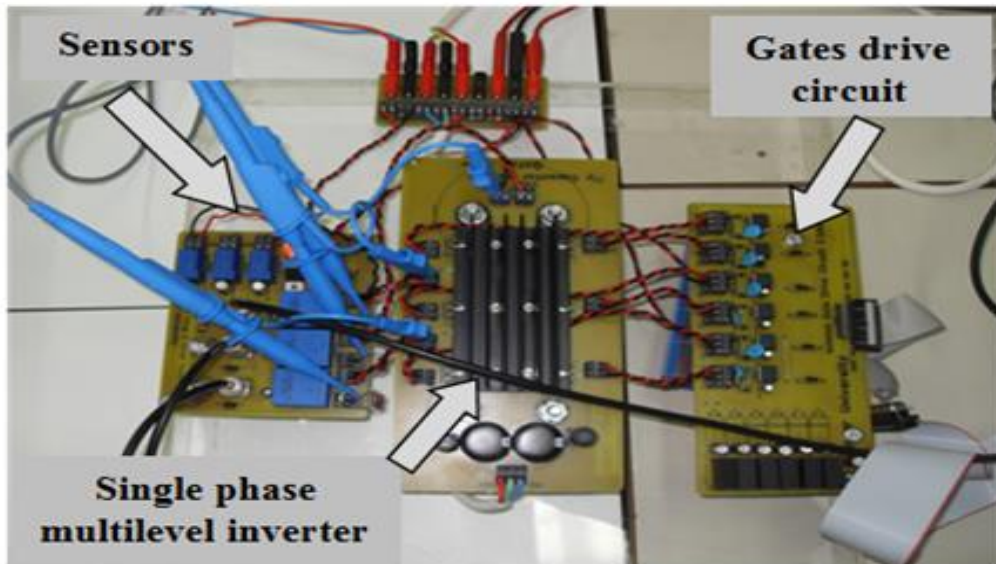


Fig. 18. Experiment set

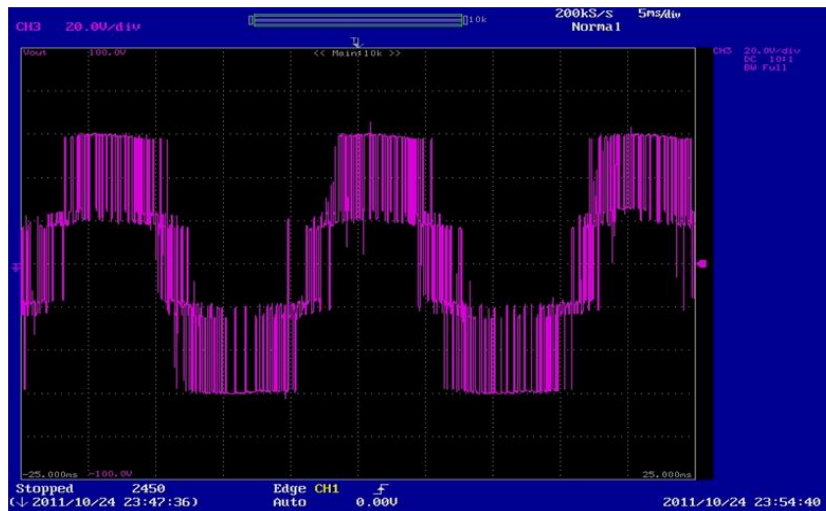


Fig. 19. Experimental output inverter voltage

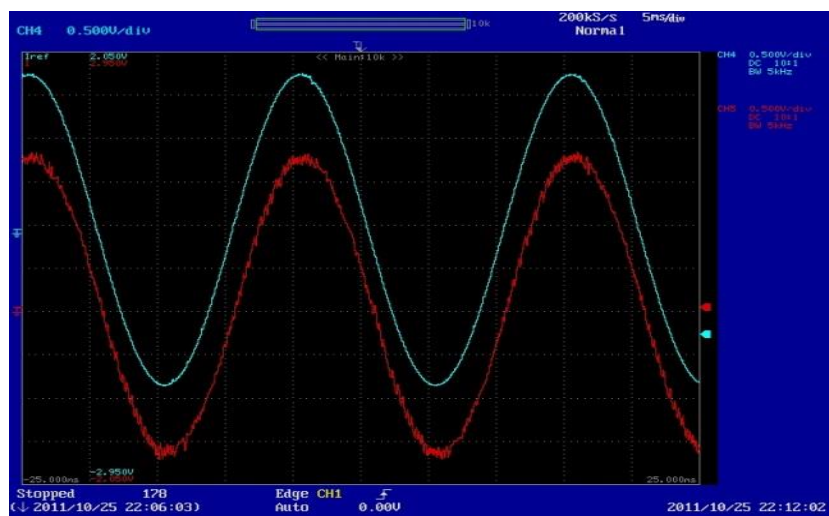


Fig. 20. Experimental output inverter & reference current

7. Conclusion

In this paper, PV grid-connected system is proposed. The performance of this system under islanding operation mode and grid voltage sags is tested. Hysteresis current control combined with active islanding detection methods (AFD, SMS) is developed to meet the Grid connection requirement (GCR) like THD, unity power factor, power quality, in one hand. In other hand, to detect island operation mode and to shut down the PV inverter when the grid is disconnected.

SPIM is taken as local load to shows the effect of grid voltage sags with different depth and durations.

An experimental multilevel inverter is also developed for the grid connection of PV generator and to verify the proposed controller.

Theoretical analysis, simulation, and experimental results show the performance of the proposed system

References

- [1] European Photovoltaic Industry Association (EPIA), Market Report 2011.
- [2] IEEE Standard for Interconnecting Distributed Resources with Electric Power Systems, IEEE Std 1547.2-2008.
- [3] M. G. Villalva, J. R. Gazoli, E. Ruppert, “Modelling and circuit-based simulation of photovoltaic arrays”, Brazilian Journal of Power Electronics, 2009, vol. 14, no. 1, ISSN 1414-8862, pp. 35-45.
- [4] M. Trabelsi, M. Brahim, K.A Ghazi, L. Ben-Brahim, S. Al-Dosari, J. Belhadj “A new design of predictive controller combined with an islanding detection method for a grid connected Photovoltaic Power Conditioning System” International Renewable Energy Congress, Tunisia, December 2011, pp.352-358.
- [5] M. Xu, R.V.N. Melnik, U. Borup, “Modeling anti-islanding protection devices for photovoltaic systems”, Elsevier on Renewable Energy 29 (2004), pp. 2195-2216.

- [6] L.A.C. Lopes, H. Sun, "Performance assessment of active frequency drifting islanding detection methods", IEEE Transaction on Energy Conversion, Vol.21, No.1, March 2006, pp. 171-180.
- [7] Z. Ye, A. Kowalkar, Y. Zhang, P. Du, and R. Walling, "Evaluation of anti-islanding schemes based on non-detection zone concept," IEEE Trans. Power Electron. (2004), vol. 19, no. 5, pp. 1171-1176.
- [8] M.E. Ropp, M. Begovic, A. Rohatgi, "Determining the Relative Effectiveness of Islanding Detection Methods Using Phase Criteria and Non-detection Zones", IEEE Transactions on Energy Conversion, Vol. 15, No. 3, September 2000, pp. 290-296.
- [9] M. H. J. Bollen "Understanding Power Quality Problems. Voltage sags and interruptions", IEEE Press Series on Power Engineering, 2000, ISBN 0-7803- 4713-7.
- [10] S.B.Kjaer, J. K. Pedersen, and F. Blaabjerg, "A Review of Single-Phase Grid-Connected Inverters for Photovoltaic Modules", IEEE Transaction On Industry Applications", Vol. 41, No. 5, September/October 2005, pp . 1292-1306.
- [11] F. Blaabjerg, R. Teodorescu, M. Liserre, and A.V. Timbus," Overview of Control and Grid Synchronization for Distributed Power Generation Systems", IEEE Transaction on Industrial Electronics, Vol. 53, No. 3, June 2001, pp. 594-601.
- [12] R.A. Mastromauro, M. Liserre, T. Kerekes, and A. Aquila " A Single-Phase Voltage-Controlled Grid-Connected Photovoltaic System With Power Quality Conditioner Functionality", IEEE Transaction on Industrial Electronics, Vol. 56, No. 11, November 2009, pp. 4436-4444.
- [13] J. H. R. Enslin, M. S.Wolf, D. B. Snyman, and W. Sweigers," Integrated photovoltaic maximum power point tracking converter", IEEE Transaction on Industrial Electronics, vol. 44 , Dec. 1997, pp. 769-773.
- [14] M.F.McGranaghan, D.R. Mueller, M.J.Samotyj," Voltage sags in industrial systems" IEEE Transaction On Industry Applications, Vol. 29, No 2, Mars-April 1993, pp.397-403.
- [15] J.-W. Choi, Y.-K. Kim and H.-G. Kim, "Digital PLL control for single-phase photovoltaic system," Proc. IEEE, Elect. Power Appl., Vol. 153, No. 1, Jan. 2006, pp. 40-46.
- [16] L. Asiminoaei, R.Teodorescu, F. Blaabjerg, and U. Borup," Implementation and Test of an Online Embedded Grid Impedance Estimation Technique for PV Inverters" IEEE Transaction on Industrial Electronics, Vol. 52, No. 4, August 2005, pp. 1136-1144.